



Contents lists available at ScienceDirect

Catalysis Today

journal homepage: www.elsevier.com/locate/cattod



Fischer Tropsch Synthesis using promoted cobalt-based catalysts

Sarwat Iqbal^a, Thomas E. Davies^a, James S. Hayward^a, David J. Morgan^a, Khalid Karim^b, Jonathan K. Bartley^a, Stuart H. Taylor^a, Graham J. Hutchings^{a,*}

^a Cardiff Catalysis Institute, School of Chemistry, Cardiff University, Main Building, Park Place, Cardiff CF10 3AT, UK

^b SABIC Technology and Innovation, P.O. Box 42503, Riyadh 11551, Saudi Arabia

ARTICLE INFO

Article history:

Received 6 April 2016

Accepted 7 April 2016

Available online xxx

Keywords:

Fischer Tropsch Synthesis

CoMnO_x

Promoters

Lanthanum

Phosphorus

Syngas

ABSTRACT

A series of CoMnO_x catalysts with lanthanum and phosphorus promoters were prepared by wet impregnation and investigated for syngas conversion to hydrocarbons activity via Fischer Tropsch Synthesis. The effects of the promoters on the catalyst structure were examined by ICP, XRD, TPR and XPS measurements. The results of the catalytic tests showed that the addition of promoters altered the product selectivities when compared to the unpromoted catalyst.

© 2016 Elsevier B.V. All rights reserved.

1. Introduction

Fischer Tropsch Synthesis (FTS) is an important process for the synthesis of hydrocarbons from syngas mixtures (CO + H₂). Recently interest in FTS has increased as a promising alternative process for the production of low-sulphur fuels from the conversion of syngas.

CoMnO_x catalysts have been extensively studied for the conversion of syngas to light hydrocarbons, due to their relatively low selectivity towards CO₂ and CH₄ [1–3]. Further to this, the addition of rare-earth metals into Co-based catalysts has been reported to be beneficial in FTS [4,5], and the promotional effect of lanthanum on supported metal oxides in particular has been widely studied. Barraut et al. [5] reported an increase in specific activity for FTS by the addition of a La promoter to supported Co catalysts. A La/Co/Al₂O₃ catalyst system was studied by Vada et al. [4], and it was observed that low loading of La (La/Co = 0.05) increased the overall catalytic activity in the FTS reaction. The effect of La addition on the properties of precipitated metal oxides, such as Fe-based catalysts, has also been reported [6]. Haddad et al. [7] performed a characterization study of La-promoted Co/SiO₂ systems and showed that La(III) can regulate the strong Co-support interactions and the reducibility of Co oxide.

In addition to the promotional effect of rare earth metals, some studies have also shown a profound promotion effect from the addition of group 15 elements, particularly phosphorus on supported metal oxides for the FTS reaction [8–10]. Bae et al. [11] reported an increase in FTS activity and C₅₊ selectivity by modification of a Co/Al₂O₃ catalyst by the addition of an appropriate amount of phosphorus (1–2 wt%). Other studies have reported an increase in the reducibility of cobalt species, which was shown to have originated from the weak interaction between cobalt and the phosphorus-modified surface. This weak interaction arises from the partial transformation of the Al₂O₃ surface to aluminium phosphate [12]. An increase in catalytic activity and stability has been reported by promotion of a Ru/Co/SiO₂ catalyst with Zr and P. Addition of an appropriate amount of Zr and P into the oxide supported catalyst was postulated to have prevented the cobalt particle aggregation and enhanced the stability of the catalyst [13].

Although a significant amount of work regarding the effect of La and/or P promoter on Co based FTS catalysts has been reported, the main focus has been on Al₂O₃, SiO₂, TiO₂, and activated carbon supported catalysts. However, it appears that no study in the open literature has been devoted to the effect of these promoters on CoMnO_x catalysts. Therefore, it would be interesting to examine the impact of both La and P addition on a CoMnO_x catalyst. In the present study we have compared the effect of addition of La and P dopants on the catalytic activity of CoMnO_x catalysts. Furthermore the effect of sequential addition of both dopants to a CoMnO_x catalyst has also been studied.

* Corresponding author.

E-mail address: hutch@cardiff.ac.uk (G.J. Hutchings).

2. Experimental

2.1. Catalyst preparation

2.1.1. CoMnO_x

CoMnO_x catalysts were prepared according to the procedure used previously [8,9]. An aqueous solution was prepared containing equimolar amounts of cobalt nitrate hexahydrate ($\text{Co}(\text{NO}_3)_2 \cdot 6\text{H}_2\text{O}$, Sigma Aldrich, 99.999%) and manganese nitrate tetrahydrate ($\text{Mn}(\text{NO}_3)_2 \cdot 4\text{H}_2\text{O}$, Sigma Aldrich, $\geq 98\%$). This solution was heated to 80°C and aqueous ammonia (28–30% NH_3 in water, Sigma Aldrich) was added to raise the pH from 2.9 to 8.30 ± 0.01 . The resulting precipitate was recovered by filtration, washed with distilled water (1 dm^3 , 80°C), and dried (110°C , 16 h).

2.1.2. $\text{CoMnO}_x\text{-La}$ and $\text{CoMnO}_x\text{-P}$

The addition of La and P dopants was performed by the wet impregnation method. For the synthesis of $\text{CoMnO}_x\text{-La}$, the required amount of lanthanum nitrate ($\text{La}(\text{NO}_3)_3 \cdot 6\text{H}_2\text{O}$, Sigma Aldrich, 99.999%) was dissolved in 2 cm^3 of deionized water and stirred for approximately 15 min until a clear solution was obtained. The dried precursor form of CoMnO_x was added to the solution and stirred at room temperature to form a paste. The paste was subsequently dried (110°C , 16 h). The resulting material was calcined in static air (500°C , 24 h, with a ramp rate from ambient of $20^\circ\text{C min}^{-1}$).

$\text{CoMnO}_x\text{-P}$ catalysts were prepared by following the same method, except that ammonium phosphate ($\text{NH}_4\text{H}_2\text{PO}_4$, sigma Aldrich, 98%) was used as a phosphorus source instead of lanthanum nitrate.

2.1.3. $\text{CoMnO}_x\text{-La-P}$

In order to prepare the $\text{CoMnO}_x\text{-La-P}$ catalysts, $\text{CoMnO}_x\text{-La}$ was first prepared by wet impregnation as reported above, followed by a drying step (110°C , 16 h). In the next step the P dopant was added by wet impregnation. The resulting slurry was dried (110°C , 16 h) and calcined in static air (500°C , 24 h, and $20^\circ\text{C min}^{-1}$).

2.2. Catalytic activity

The catalysts were pelleted and sieved (0.65–0.85 mm), before samples (0.5 g) were loaded into stainless steel fixed bed reactors (internal diameter 8 mm). Catalysts were reduced *in situ* at 400°C for 16 h in pure hydrogen ($\text{GHSV} = 600 \text{ h}^{-1}$) before being allowed to cool to room temperature. The reactor was subsequently pressurized to 6 barg with syngas ($\text{CO}:\text{H}_2 = 1:1$ molar ratio). All catalysts were tested under the same reaction conditions, (240°C , 6 barg, $\text{GHSV} = 600 \text{ h}^{-1}$).

A stabilization period of ~ 100 h was allowed before catalyst data was collected and the mass balance determined. Analysis of gas products was performed by on-line gas chromatography using a Varian 3800 GC. Hydrocarbons were analysed using a CP- $\text{Al}_2\text{O}_3/\text{KCl}$ column and a flame ionisation detector. Permanent gases and $\text{C}_1\text{-C}_4$ hydrocarbons were analysed using molecular sieve 13X and Poropak Q columns with TCD and FID detectors in series. The product stream was cooled in a wax trap ($\sim 25^\circ\text{C}$) to retain the liquid products. Calibrations were performed with standard samples ($\text{C}_1\text{-C}_5$ hydrocarbon mixture diluted with nitrogen, BOC certified) for data quantification. Nitrogen was used as an internal standard to correct for contraction of the gas volume following reaction.

2.3. Catalyst characterization

2.3.1. X-ray photoelectron spectroscopy (XPS)

XPS was performed using a Kratos Axis Ultra-DLD photoelectron spectrometer, using monochromatic Al $\text{K}\alpha$ radiation operating

Table 1
ICP elemental analysis of La and P content in the catalysts.

Catalysts	La content (wt%)		P content (wt%)	
	Theoretical	Measured	Theoretical	Measured
$\text{La}_{0.05}$	0.05	0.03	0	0.00
$\text{La}_{0.1}$	0.10	0.08	0	0.00
$\text{La}_{0.5}$	0.50	0.20	0	0.00
La_1	1.0	1.10	0	0.00
$\text{P}_{0.03}$	0	0.00	0.03	0.01
$\text{P}_{0.05}$	0	0.00	0.05	0.06
$\text{P}_{0.1}$	0	0.00	0.10	0.08
$\text{La}_{0.1}\text{-P}_{0.03}$	0.1	0.07	0.03	0.01
$\text{La}_{0.1}\text{-P}_{0.05}$	0.1	0.13	0.05	0.02

at 144 W ($12 \text{ mA} \times 12 \text{ kV}$). High resolution and survey scans were performed at pass energies of 40 and 160 eV respectively. Spectra were calibrated to the C (1s) signal at 284.8 eV, and quantified using CasaXPS v2.3.17, utilizing sensitivity factors supplied by the manufacturer.

2.3.2. Powder X-ray diffraction (XRD)

Powder X-ray diffraction (XRD) was performed on a X'Pert Pro diffractometer with a monochromatic Cu- $\text{K}\alpha$ source ($\lambda = 0.154 \text{ nm}$) operated at 40 kV and 40 mA. Data were collected over a 2θ range from 10° to 80° , and phases identified by matching with the ICDD database.

2.3.3. Temperature programmed reduction (TPR)

Temperature programmed reduction/oxidation was carried out using a TPDRO 1100 series analyser. Samples (25 mg) were pre-treated for 1 h at 130°C ($20^\circ\text{C min}^{-1}$) in a flow of Argon ($20 \text{ cm}^3 \text{ min}^{-1}$). Following this the gas flow was changed to 10% H_2/Ar and the temperature was ramped to 800°C ($10^\circ\text{C min}^{-1}$) with a 5 min hold at the T_{max} . H_2/O_2 consumption was monitored using a TCD detector.

2.3.4. Inductively Coupled Plasma (ICP-AES)

Catalyst bulk elemental composition was determined by Inductively Coupled Plasma (ICP) (ICPE-9000, Shimadzu). 25 mg of the calcined catalyst was dissolved in 0.5 cm^3 of *aqua regia* at room temperature overnight. The solutions obtained were diluted with distilled water up to 10 ml. The prepared solutions were subjected to ICP analysis. For calibration, standard solutions of 1000 ppm of La and 1000 ppm of P were mixed and diluted to 0.2, 0.5, 1.0, 2.5, and 5.0 ppm.

Analysis showed that the amounts of dopant were in general agreement with the theoretical amounts. The error in P content was consistently within $\pm 0.03 \text{ wt}\%$, and the error in La content was within $\pm 0.02 \text{ wt}\%$. One exception to this was $\text{La}_{0.5}$, which had an error of $-0.3 \text{ wt}\%$. The full data are shown in Table 1.

3. Results and discussion

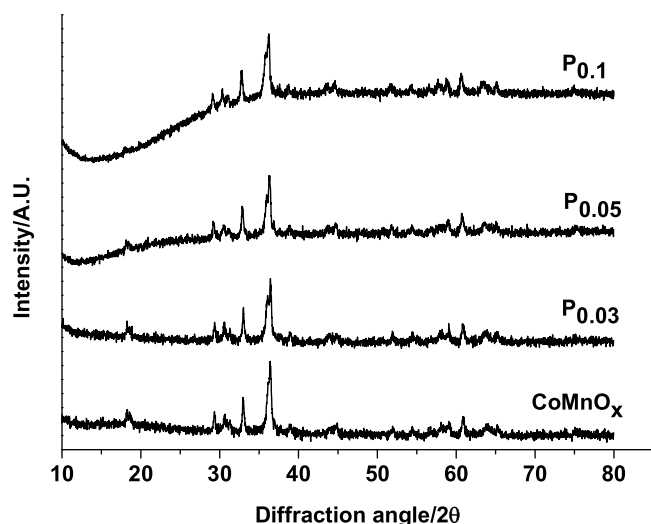
3.1. $\text{CoMnO}_x\text{-P}$

The catalysts doped with various loadings of P were tested for FTS activity under identical conditions and the results are presented in Table 2. A comparison of the CoMnO_x and $\text{CoMnO}_x\text{-P}$ catalyst performance indicates that all the P doped catalysts showed a lower CO conversion and CO_2 selectivity. The addition of phosphorus increased the selectivity to alkenes particularly propene and butene. It was apparent that increasing the phosphorus content decreased the selectivity to alkenes, and increased the CH_4 selectivity. All of these catalysts required around 90 h to stabilize and no deactivation was observed after the stabilization was achieved during the period of our investigation. The deactivation of the catalyst

Table 2
Effect of addition of P promoter on FTS activity of CoMnO_x catalyst.

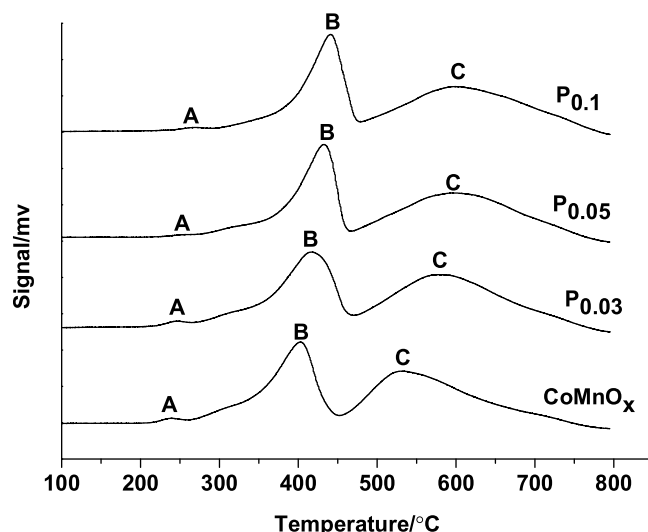
	CoMnO _x	CoMnO _x -P _{0.03}	CoMnO _x -P _{0.05}	CoMnO _x -P _{0.1}
CO conversion (%)	35.5	30	31	25.8
Product selectivity (%)				
CH ₄	22.1	17.0	19.0	25.0
C ₂ -C ₄	17.2	37.0	40.9	32.8
C ₅ +	17.0	17.0	19.0	17.0
CO ₂	37.0	27.0	21.0	25.0
Alcohols	6.7	2.0	0.1	0.2

Reaction conditions: Catalyst 0.5 g, 240 °C, data collected at 110 h, 6 Barg, CO:H₂ 1:1 mol ratio, GHSV 600 h⁻¹.

**Fig. 1.** XRD pattern of P doped catalysts.

by the addition of P runs contrary to the literature on phosphorus promotion in Co/Al₂O₃ [11–13]. However, it should be noted that the promotion effect in all previous studies was concluded to stem from the formation of a weakly-interacting aluminium phosphate support phase. In this study, where no support is used and the phosphorus is directly applied to the surface of the catalyst, the P does not act as a promoter, instead it appears to act by blocking access to the active sites.

All catalysts doped with P were characterised by XRD and the data set is presented in Fig. 1. These catalysts showed the diffraction pattern for the mixed Co and Mn spinel oxide (with an intermediate tetragonal structure between CoMn₂O₄ and Mn₃O₄) (ICDD 018-0408). The characteristic reflections of mixed CoMn₂O₄ phases remained at the same position upon impregnation of P at all levels. No reflections associated with the P containing components were observed. Small shoulders were visible on the lower-angle side of the main reflection at 36.06°. It is difficult to directly assign these reflections, as reflections will occur in this region for CoO, Co₃O₄, Mn₃O₄ and CoMn₂O₄. Whilst the overall pattern is one of the mixed metal spinel structure, the potential overlap of reflections makes it difficult to definitively state the full phase composition. XRD analysis was unable to resolve any structural differences between any of

**Fig. 2.** TPR profiles of P-doped CoMnO_x catalysts.

the catalysts. This is likely due to the low amounts of the promoter present, and also due to their addition on to the surface, as opposed to incorporation into the bulk structure.

The TPR profiles and the corresponding data of the CoMnO_x and CoMnO_x-P doped catalysts are displayed in Fig. 2 and Table 3. For each catalyst two distinct reduction signals could be observed with a small signal at lower temperature. The first signal at 240–260 °C (A) is assigned to the reduction of Co(III) to Co(II); this would seem to imply the presence of at least some Co₃O₄ in the material. Based on this, it is probably that the shoulders observed in the XRD at an angle of 36.06° can be assigned to discrete cobalt oxide phases. The second TPR signal observed between 400 and 440 °C (B) can be assigned to the reduction of Co(II) to Co(0) [14,15]. The third signal (C) is attributed to the subsequent reduction of the oxides of manganese [15,16].

Results of H₂-TPR showed that even the lowest loading (P_{0.03}) of P promoter on CoMnO_x could greatly influence the reduction temperature of Co and Mn oxides. The addition of 0.03% P to CoMnO_x resulted in an increase in the reduction temperature of both Co and Mn oxide phases. Further increase in the amount of P to 0.05% showed further increase in the reduction of Co(II) oxide signal by 16 °C and also the reduction temperature of manganese oxide (C) was increased by 22 °C. P_{0.1} showed a slight increase in the reduction temperature of Co(II) and almost no change in the Mn oxide reduction signal. The general trend was that increasing the amount of phosphorus dopant increased the reduction temperatures of all the observed signals. A decline in the reducibility of both oxides was obvious; since the activity of cobalt catalysts for FTS is linked to the reducibility, this is thought to have contributed to a loss in the catalytic activity.

Hydrogen consumption data for each reduction signal is presented in Table 3. The quantity of hydrogen consumed for the reduction of Co(II) to Co(0) was found to be similar for all the P-doped catalysts, but the hydrogen consumption for Mn oxide

Table 3
Reduction data from TPR analysis of the P-doped CoMnO_x catalysts.

Catalysts	Signal A (°C)	Hydrogen consumption (μmol/g)	Signal B (°C)	Hydrogen consumption (μmol/g)	Signal C (°C)	Hydrogen consumption (μmol/g)
CoMnO _x	239	33	402	2551	530	3435
P _{0.03}	239	33	418	2545	577	3705
P _{0.05}	254	10	434	2588	599	3279
P _{0.1}	267	21	439	2538	597	2865

Table 4
XPS derived molar concentrations for undoped and P-doped CoMnO_x catalysts.

Catalysts	Concentration/at%				Co/Mn	Co + Mn/O _{Lattice}
	Co (2p)	Mn (2p)	O (1s)	P (2p)		
CoMnO _x	15.34	23.2	61.46	0	0.66	0.76
P _{0.03}	15.05	22.07	62.03	0.85	0.68	0.78
P _{0.05}	14.81	21.92	62.05	1.22	0.68	0.78
P _{0.1}	13.48	21.58	62.74	2.2	0.62	0.80

reduction increased for P_{0.03} and then decreased with the addition of more P into CoMnO_x catalyst.

To ascertain the concentration and oxidation states of the synthesised catalysts, XPS analysis was performed and the derived molar ratios are given in Table 4. For clarity the molar ratios have been corrected for the adventitious carbon. For the undoped CoMnO_x catalyst the Mn(2p_{3/2}) and Co(2p_{3/2}) binding energies were 642.2 eV and 780.6 eV respectively; the latter is characteristic of cobalt in Co–Mn mixed metal oxides [17] and CoO [18–20] with the satellite structure encompassing the energy range ca. 785–790 eV due to the 3d → 4s shake-up process and suggests the presence of Co(II).

The Mn binding energies were more difficult to directly assign due to the similarity in binding energies of Mn compounds and potentially weak satellite structure which may aid elucidation [20], however the multiplet splitting of the Mn(3s) signal maybe used to further ascertain the nature of the Mn species and here was measured at 5.4 (± 0.2) eV suggestive of Mn(III).

The surface of the undoped sample also comprised of adventitious carbon and small amounts of carbonate and hydroxide, as evidenced by the asymmetry of the O(1s) signal to the high binding energy side (not shown). Fitting of the lattice oxygen and hydroxide/C–O species revealed a (Co + Mn)/O ratio of 0.76 in excellent agreement with the bulk stoichiometry expected for tetragonal CoMn₂O₄ (i.e. 0.75). However, the Co/Mn ratio is slightly higher than that expected from the bulk stoichiometry possibly suggesting some segregation of cobalt oxide in the near surface region.

Table 4 shows the molar concentrations of the P-doped samples. Phosphorus was characterised by a binding energy of 133.3 eV, characteristic of phosphate (PO₄³⁻) or pyrophosphate (P₂O₇⁴⁻) [20]. The Co and Mn (2p) spectra were identical in energy and shape to that of the undoped sample whilst the combined metal to lattice oxygen ratio was slightly higher than that of the undoped CoMnO_x (ca. 0.80 vs 0.76).

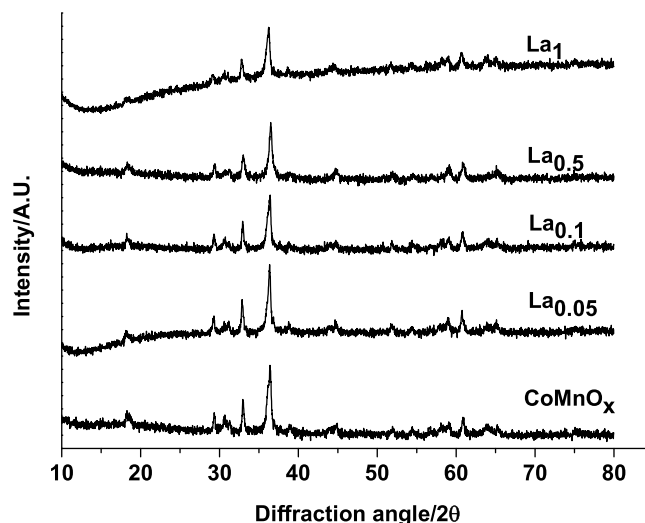
3.2. CoMnO_x-La

The catalysts doped with various loadings of lanthanum were tested for FTS activity under identical conditions and the data are presented in Table 5. All the La-doped catalysts displayed lower CO conversion, lower selectivity to CO₂ and higher selectivity to alkenes. The selectivity to CO₂ and CH₄ was decreased markedly for a lower loading of La (0.05 and 0.1%). A further increase in La

Table 5
Effect of addition of La promoter on FTS activity of CoMnO_x catalyst.

	CoMnO _x	CoMnO _x -La _{0.05}	CoMnO _x -La _{0.1}	CoMnO _x -La _{0.5}	CoMnO _x -La ₁
CO conversion (%)	36	33	31	21.8	18.8
Product selectivity (%)					
CH ₄	22.1	17.0	15.0	21.7	26
C ₂ -C ₄	17.2	27.0	37.6	31.0	20.5
C ₅ +	17.0	31.0	28.0	15.0	13.5
CO ₂	37.0	24.5	19.0	31.0	38.5
Alcohols	6.7	0.3	0.4	1.3	1.9

Reaction conditions: Catalyst 0.5 g, 240 °C, data collected at 130 h, 6 Barg, CO:H₂ 1:1 mol ratio, GHSV 600 h⁻¹.

**Fig. 3.** XRD pattern of La doped catalysts.**Table 6**
XPS derived molar concentrations for La-doped CoMnO_x catalysts.

Catalysts	Concentration/at%				Co/Mn	Co + Mn/O _{Lattice}
	Co (2p)	Mn (2p)	O (1s)	La (3d)		
La _{0.05}	16.48	22.31	60.86	0.36	0.74	0.78
La _{0.1}	14.90	22.78	62.03	0.28	0.65	0.79
La _{0.5}	12.05	24.27	62.11	1.57	0.50	0.75
La _{1.0}	12.31	22.44	63.31	1.94	0.55	0.68

up to 0.5 and 1% showed a significant decline in the CO conversion and also the selectivity to methane and carbon dioxide increased markedly. The decrease in CO conversion upon addition of La into the CoMnO_x catalyst and a shift of the selectivity towards lower carbon-number products is similar to the effects of potassium doping, in which the dopant blocks CO dissociating sites [21]. Lowering the dissociative ability of the catalyst would cause the effects observed. The addition of phosphorus appears to have a similar effect, although it was less pronounced; it is possible that the lanthanum is selectively binding to certain sites, whereas the acidic phosphorus is non-selectively blocking the surface. This is somewhat in agreement with the conclusions of Prieto et al. [22].

The XRD patterns of CoMnO_x-La catalysts are shown in Fig. 3. All of the La doped catalysts were found to be very similar to the pure CoMnO_x catalyst; no additional phases were observed and the reflections remained at the same position. All the catalysts showed the diffraction pattern for the mixed spinel oxide of Co and Mn (with an intermediate tetragonal structure between CoMn₂O₄ and Mn₃O₄) (ICDD 018-0408).

Surface molar concentrations of the elements present for the CoMnO_x-La catalysts, derived by XPS, are presented in Table 6. The analysis revealed the La to be present in its 3+ state with a

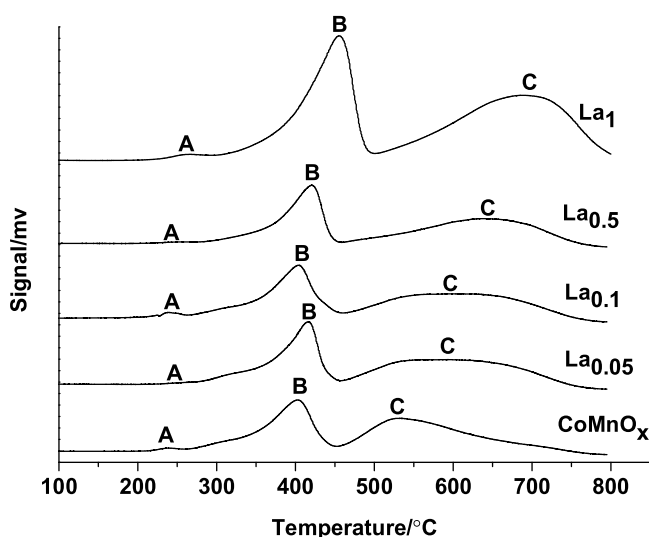
Table 7
Reduction data from TPR analysis of the La-doped catalysts.

	Signal A (°C)	Hydrogen consumption (μmol/g)	Signal B (°C)	Hydrogen consumption (μmol/g)	Signal C (°C)	Hydrogen consumption (μmol/g)
CoMnO _x	238	32	401	2557	537	3633
La _{0.05}	241	13	416	2711	582	3994
La _{0.1}	246	48	402	2534	594	3592
La _{0.5}	251	77	421	2503	643	3566
La ₁	265	35	455	2628	685	3528

La(3d_{5/2}) binding energy of 834.6 eV characteristic of La₂O₃. For the La-doped samples the Mn region remains consistent with that of the un-doped spinel and consistent with the XRD data which suggests no bulk incorporation. A decrease in the amount of Co was observed with an increase in La content.

The effect of La addition on the reduction profile of La-doped catalysts is shown in Fig. 4 and Table 7. Addition of 0.05% La into CoMnO_x increased the reduction temperature of Co(II) (B) by 15 °C and a shift of 45 °C towards higher temperature was observed in the reduction temperature of Mn oxide (C). Further addition of 0.1 and 0.5% La further increased the reduction temperature of Co oxide and Mn oxide reduction signals. The catalyst doped with 1% La showed the highest reduction temperature amongst the series of La doped catalysts for the reduction of both Co(II) and Mn oxide reduction signals. Hydrogen consumption data for La-doped catalysts showed a very little change in the reduction signal of Co(II). The amount of hydrogen consumed for Mn oxide reduction increased with an addition of 0.05% La and decreased on further addition of La.

It has been reported that La addition into the supported Co catalysts can facilitate the cobalt oxide reduction, particularly for the Co(II) to Co(0) which provides more cobalt active sites and therefore an increase in the catalytic activity [23]. However, we have observed an increase in the reduction temperature with an addition of La promoter into CoMnO_x catalyst, and hence a significant loss of catalytic activity. The blocking of CO dissociative sites is possible with La addition as previously reported for potassium promoters [21,24], which can lead to a loss in catalytic activity. Increasing the La loading on the catalysts lowered the surface concentration of Co implying that the La is primarily positioning itself on the cobalt surface, which is in agreement with the theory that it is selectively blocking the CO dissociation sites on the cobalt in a manner similar to potassium.

**Fig. 4.** TPR profiles of La-doped CoMnO_x catalysts.**Table 8**
Effect of a combined addition of La and P promoters on CoMnO_x.

	CoMnO _x -La _{0.1}	CoMnO _x -La _{0.1} -P _{0.03}	CoMnO _x -La _{0.1} -P _{0.05}
CO conversion (%)	31	29.8	29.0
Product selectivity (%)			
CH ₄	15.0	11.0	13.7
C ₂ -C ₄	37.6	46.5	52.0
C ₅ +	28.0	26.0	19.0
CO ₂	19.0	14.5	13.0
Alcohols	0.4	2.0	2.3

Reaction conditions: Catalyst 0.5 g, 240 °C, data collected at 110 h, 6 Barg, CO:H₂ 1:1 mol ratio, GHSV 600 h⁻¹.

3.3. CoMnO_x-La-P

The catalysts doped both with La and P were tested and the catalytic data is presented in Table 8. The catalyst prepared with the sequential addition of 0.1% of La and 0.03% of P showed a significant increase in the selectivity towards alkenes and a lower CO conversion compared with the CoMnO_x-La_{0.1} catalyst. This catalyst also showed low selectivities to CH₄ and CO₂. Further increase in the amount of P to 0.05% showed a comparable product spectrum and the same activity as P_{0.03} catalyst.

The XRD patterns of CoMnO_x-La-P are shown in Fig. 5. Both of these catalysts were found to be similar to the P-doped catalysts. The characteristic reflections of CoMn₂O₄ did not show any shift in their position on addition of dopants. Again like P and La doped catalysts, no phases associated with the P or La were observed. As before, shoulder reflections can be observed, and are tentatively assigned to Co₃O₄.

The TPR profiles and the corresponding data are shown in Fig. 6 and Table 9. As was seen with the CoMnO_x-P series of catalysts, increasing the loading of the phosphorus promoter has increased the reduction temperature of both the Co(II) and Mn(x) reduction

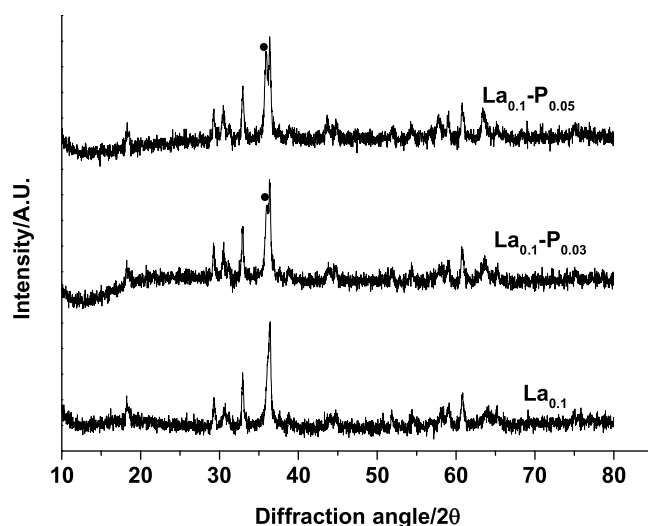
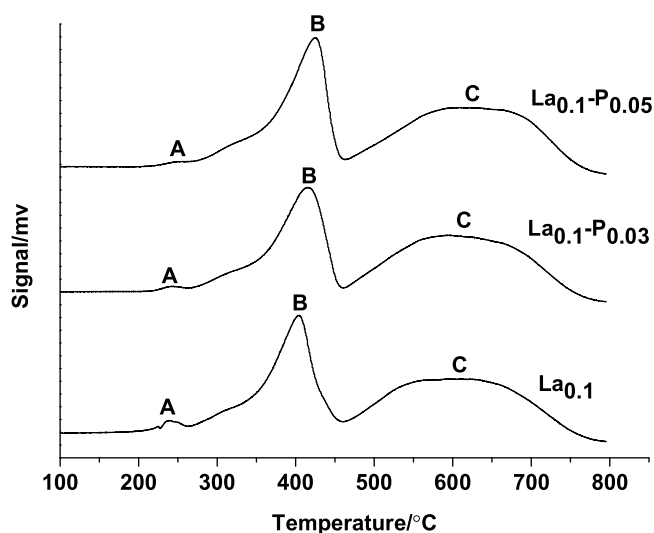
**Fig. 5.** XRD pattern of La and P doped catalysts; ● Co₃O₄.

Table 9
Reduction data from TPR analysis of the La-P-doped catalysts.

Catalysts	Signal A (°C)	Hydrogen consumption (μmol/g)	Signal B (°C)	Hydrogen consumption (μmol/g)	Signal C (°C)	Hydrogen consumption (μmol/g)
La _{0.1}	246	47	402	2534	594	3593
La _{0.1} -P _{0.03}	240	24	418	2654	604	4149
La _{0.1} -P _{0.05}	239	17	425	2922	621	3669

Table 10
XPS derived molar concentrations for La and P-doped CoMnO_x catalysts.

Catalysts	Concentration/at%					Co/Mn	Co + Mn/O _{Lattice}
	Co (2p)	Mn (2p)	O (1s)	La (3d)	P (2p)		
La _{0.1} -P _{0.03}	14.35	22.44	62.13	0.34	0.74	0.64	0.77
La _{0.1} -P _{0.05}	14.13	22.05	62.2	0.63	0.99	0.64	0.78

**Fig. 6.** TPR profiles of La-P-doped CoMnO_x catalysts.

signals. La_{0.1}-P_{0.03} catalyst showed a Co oxide reduction at the same temperature as P_{0.03} but at a higher temperature (by 16 °C) compared with La_{0.1}. Mn oxide reduction signal showed a shift towards higher temperature compared with both P_{0.03} and La_{0.1} catalysts. Further increase in the amount of P from 0.03 to 0.05% (into La doped catalyst) increased the reduction temperature of Co(II) by 7 °C and also a shift towards higher temperature was observed in the reduction signal of Mn oxide by 17 °C. Hydrogen consumption for the reduction of Co(II) increased with an addition of P into La doped CoMnO_x catalyst and for Mn oxide species first increased then decreased with further increase in the amount of P.

XPS analysis of the samples again revealed consistent Co/Mn/O ratios, however, surprisingly despite the lanthanum content being kept constant in the preparation, the increase in phosphorus seemingly has an effect of doubling the apparent amount of La (Table 10). This cannot be attributed to the formation of discrete La₂O₃ and LaPO₄ as the La(III) binding energy for the latter would be ca. 1 eV higher than that reported herein and therefore suggests the La maybe better dispersed by the increased phosphorus content.

4. Conclusions

We have investigated and contrasted the effect of La and P dopants on cobalt manganese oxide (CoMnO_x) catalyst for FTS

activity. When La and P added were added by impregnation to the CoMnO_x catalyst an increased selectivity to hydrocarbons was observed and the selectivity to CH₄ and CO₂ was decreased in comparison to the undoped CoMnO_x catalyst. In addition a considerable decrease in CO conversion was observed. La appears to selectively block Co sites on the surface, and promotes the formation of lower carbon number products.

Acknowledgement

We would like to thank Sabic for financial support.

References

- [1] M. Van der Riet, G.J. Hutchings, R.G. Copperthwaite, *J. Chem. Soc. Chem. Commun.* 10 (1986) 798–799.
- [2] R.G. Copperthwaite, G.J. Hutchings, M. Van der Riet, *J. Woodhouse, Ind. Eng. Chem. Res.* 26 (1987) 869–874.
- [3] A.P. Hindermann, G.J. Hutchings, A. Kiennemann, *Catal. Rev. Sci. Eng.* 35 (1993) 19–35.
- [4] S. Vada, B. Chen, J.G. Goodwin, *J. Catal.* 153 (1995) 224–231.
- [5] J. Barrault, A. Guilleminot, J.C. Achard, V. Paul-Boncour, A. Percheron-Guegan, *Appl. Catal.* 21 (1986) 307–312.
- [6] D. Wang, X. Cheng, Z. Huang, X. Wang, S. Peng, *Appl. Catal.* 77 (1991) 109–122.
- [7] G.J. Haddad, B. Chen, J.G. Goodwin Jr., *J. Catal.* 160 (1996) 43–51.
- [8] K. Karim, M. Al-Semahi, A. Khan, (2014) WO 2014001354.
- [9] K. Karim, S.A. Al-Sayari, (2012), WO 2012084160.
- [10] S.J. Park, J.W. Bae, G.-I. Jung, K.-S. Ha, K.-W. Jun, Y.-J. Lee, H.-G. Park, *Appl. Catal. A* 413–414 (2012) 310–321.
- [11] J.W. Bae, S.-M. Kim, Y.-J. Lee, M.-J. Lee, K.-W. Jun, *Catal. Commun.* 10 (2009) 1358–1362.
- [12] M.H. Woo, J.M. Cho, K.-W. Jun, Y.J. Lee, J.W. Bae, *ChemCatChem* 7 (2015) 1460–1469.
- [13] J.-W. Bae, S.-J. Park, M.-H. Woo, J.-Y. Cheon, K.-S. Ha, K.-W. Jun, D.-H. Lee, H.-M. Jung, *ChemCatChem* 3 (2011) 1342–1347.
- [14] R.P. Marin, S.A. Kondrat, J.R. Gallagher, D.I. Enache, P. Smith, P. Boldrin, T.E. Davies, J.K. Bartley, G.B. Combes, P.B. Williams, S.H. Taylor, J.B. Claridge, M.J. Rosseinsky, G.J. Hutchings, *ACS Catal.* 3 (2013) 764–772.
- [15] D.G. Klissurski, E.L. Uzunova, *Appl. Surf. Sci.* 214 (2003) 370–374.
- [16] F.C. Buciuman, F. Patcas, T. Hahn, *Chem. Eng. Process.* 38 (1999) 563–569.
- [17] J. Ajay, M. Dattakumar, S. Anil, J.M. Sameer, S. Parvez, B. Narayan, O. Satishchandra, R.V. Chandrashekhara, *Catal. Sci. Technol.* 4 (2014) 1771–1778.
- [18] M. Oku, K. Hirokawa, *J. Electron. Spectrosc. Relat. Phenom.* 8 (1976) 475–481.
- [19] T.J. Chuang, C.R. Brundle, D.W. Rice, *Surf. Sci.* 59 (1976) 413–429.
- [20] M.C. Biesinger, B.P. Payne, A.P. Grosvenor, L.W.M. Lau, A.R. Gerson, R.S.C. Smart, *Appl. Surf. Sci.* 257 (2011) 2717–2730.
- [21] V.R.R. Pendyala, U.M. Graham, G. Jacobs, H. B. Davis, *Catal. Lett.* 144 (2014) 1704–1716.
- [22] G. Prieto, M.I.S. De Mello, P. Concepcion, R. Murciano, S.B.C. Pergher, A. Martinez, *ACS Catal.* 5 (2015) 3323–3335.
- [23] Y. Zhang, K. Liew, J. Li, X. Zhan, *Catal. Lett.* 139 (2010) 1–6.
- [24] D.G. Miller, M. Moskovits, *J. Phys. Chem.* 92 (1988) 6081–6085.